OPTIMIZATION OF FIR FILTERS SYNTHESIZED USING THE GENERALIZED ONE-STAGE FREQUENCY-RESPONSE MASKING APPROACH

Murat Kapar, Cercis Ö. Solmaz, and Ahmet H. Kayran

Department of Electronics and Communication Engineering, Istanbul Technical University
Maslak, 34469, Istanbul, Turkey
phone: + (90) 212 285 3609, email: kaparm@itu.edu.tr, {cercis, kayran}@ehb.itu.edu.tr

ABSTRACT

Frequency-response masking (FRM) approach is an efficient technique for significantly reducing the number of multipliers and adders in implementing sharp linear-phase finite-impulse-response (FIR) digital filters. It has been shown that further savings in arithmetic operations can be achieved by using the generalized FRM approach where the masking filters have a new structure. In both the original and the generalized synthesis techniques, the subfilters in the overall implementation are designed separately. The arithmetic complexity in the original one-stage FRM approach has been considerably reduced by using a two-step technique for simultaneously optimizing all the subfilters. Such an efficient algorithm was also proposed for synthesizing multistage FRM filters. In this paper, the two-step optimization algorithm proposed for the multistage FRM approach is adapted to the generalized one-stage FRM filters. An example taken from the literature illustrates the efficiency of the proposed technique.

1. INTRODUCTION

One of the most efficient techniques for synthesizing sharp linear-phase finite-impulse-response (FIR) digital filters with a significantly reduced number of multipliers and adders compared to the conventional direct-form implementation is the frequency-response masking (FRM) approach [1-3]. The price paid for these reductions is a slight increase in the overall filter order. The arithmetic complexity can be decreased by 20 percent or more compared with the original FRM approach by using the generalized FRM approach [4] where the two masking filters are interpolated and high-frequency components are removed by a simple filter. However, it is best suited to synthesize narrowband sharp filters.

A disadvantage of both the original and the generalized FRM synthesis techniques is that the subfilters have been designed separately. In [5], a two-step technique was proposed for simultaneously optimizing all the subfilters in the original one-stage FRM approach. A similar technique [6] has also been developed for the original multistage FRM approach. This paper exploits how to adapt the two-step optimization algorithm proposed in [6] to the generalized one-stage FRM filters. An example taken from the literature illustrates that both the number of multipliers and adders for the resulting filters are approximately 60 percent compared with those of the filters designed using the original one-stage FRM technique.

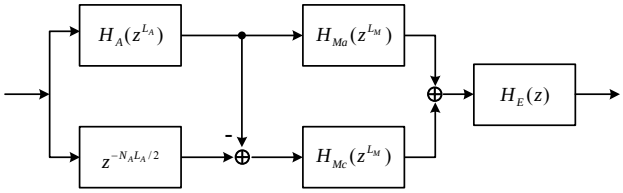

Figure 1 - Block diagram of the generalized one-stage FRM approach.

2. GENERALIZED ONE-STAGE FRM APPROACH

This section briefly reviews how to use the generalized one-stage FRM approach for designing linear-phase FIR digital filters.

2.1 Filter Structure and Frequency Response

The basic structure of the generalized one-stage FRM approach is shown in Figure 1. In this approach, the transfer function of a linear-phase FIR digital filter is constructed as follows:

$$H(z) = [H_A(z^{L_A})H_{Ma}(z^{L_M}) + H_C(z^{L_A})H_{Mc}(z^{L_M})]H_E(z), \quad (1a)$$

where

$$H_A(z^{L_A}) = \sum_{n=0}^{N_A} h_A(n) z^{-nL_A}, \quad H_C(z^{L_A}) = z^{-N_A L_A/2} - H_A(z^{L_A}), \quad (1b)$$

$$H_{Ma}(z^{L_M}) = z^{-M_{Ma}L_M} \sum_{n=0}^{N_{Ma}} h_{Ma}(n) z^{-nL_M}, \quad (1c)$$

$$H_{Mc}(z^{L_M}) = z^{-M_{Mc}L_M} \sum_{n=0}^{N_{Mc}} h_{Mc}(n) z^{-nL_M}, \quad (1d)$$

$$H_E(z) = \sum_{n=0}^{N_E} h_E(n) z^{-n}. \quad (1e)$$

Here, $h_A(n)$, $h_{Ma}(n)$, $h_{Mc}(n)$, and $h_E(n)$ are the impulse response coefficients exploiting an even symmetry. N_A, N_{Ma}, N_{Mc}, and N_E are the orders of the corresponding subfilters. N_A is even, whereas both N_{Ma} and N_{Mc} are either even or odd. If $N_{Ma} \geq N_{Mc}$, then $M_{Ma} = 0$ and $M_{Mc} = (N_{Ma} - N_{Mc}) / 2$; and if $N_{Ma} < N_{Mc}$, then $M_{Ma} = (N_{Mc} - N_{Ma}) / 2$ and $M_{Mc} = 0$. These

selections guarantee that the group delays of both $H_{Ma}(z^{L_M})$ and $H_{Mc}(z^{L_M})$ are equal. Furthermore, both $N_{Ma}L_M$ and $N_{Mc}L_M$ products must be even to avoid half sample delays [4].

The frequency response of the overall filter can be written as

$$H(e^{j\omega}) = e^{-j(N_A L_A + \max\{N_{Ma}, N_{Mc}\}L_M + N_E)\omega/2} H(\omega). \qquad (2)$$

Here, $H(\omega)$ denotes the *zero-phase frequency response* of $H(z)$ and can be expressed as follows:

$$H(\omega) = \left[H_A(L_A\omega)H_{Ma}(L_M\omega) + H_C(L_A\omega)H_{Mc}(L_M\omega)\right]H_E(\omega), \qquad (3a)$$

where

$$H_C(L_A\omega) = 1 - H_A(L_A\omega), \qquad (3b)$$

and

$$H_K(\omega) = \begin{cases} h_K(N_K/2) + 2\sum_{n=1}^{N_K/2} h_K(N_K/2-n)\cos(n\omega), & N_K \text{ even} \\ 2\sum_{n=0}^{(N_K-1)/2} h_K[(N_K-1)/2-n]\cos[(n+0.5)\omega], & N_K \text{ odd} \end{cases} \qquad (3c)$$

for $K = A, Ma, Mc, E$. Here, K is a subscript which denotes the subfilter name, i.e. H_A, H_{Ma}, H_{Mc}, or H_E. In addition, $H_A(\omega)$, $H_{Ma}(\omega)$, $H_{Mc}(\omega)$, and $H_E(\omega)$ are the zero-phase frequency responses of the subfilters $H_A(z)$, $H_{Ma}(z)$, $H_{Mc}(z)$, and $H_E(z)$, respectively.

$H_A(z^{L_A})$ is created by replacing each delay of a linear-phase model filter, $H_A(z)$, by L_A delays. $H_C(z^{L_A})$ is the complement of $H_A(z^{L_A})$. The complementary pair, $H_A(z^{L_A})$ and $H_C(z^{L_A})$, with their zero-phase frequency responses $H_A(L_A\omega)$ and $H_C(L_A\omega) = 1 - H_A(L_A\omega)$, respectively, is shown in Figure 2(a). The zero-phase frequency responses for the two masking filters, $H_{Ma}(z)$ and $H_{Mc}(z)$, are depicted in Figure 2(b). In the original approach, the transitions of the frequency masking filters are governed by $H_A(z^{L_A})$. The interpolation factor for the model filter, namely L_A, can be quite large while designing narrow transition-band filters. In this case, the transition of the two masking filters is also very narrow, leading to high-order masking filters. To overcome this problem, in the generalized FRM approach, masking filters are synthesized with lower orders and are interpolated by a factor of L_M resulting in $H_{Ma}(z^{L_M})$ and $H_{Mc}(z^{L_M})$ whose zero-phase frequency responses are shown in Figure 2(c) [2(f)]. As seen from the figure with $L_M = 2$, $H_{Ma}(L_M\omega)$ and $H_{Mc}(L_M\omega)$ have also unwanted high-frequency components. These components can be easily removed by using a simple lowpass filter, $H_E(z)$, depicted in Figure 2(d) [2(g)]. The zero-phase frequency response of the overall filter is shown in Figure 2(e) [2(h)].

2.2 Determination of Design Parameters

Let the passband edge, stopband edge, and transition-band width of the subfilter H_K be θ_K, ϕ_K, and $\Delta_K = \phi_K - \theta_K$, respectively, for $K = A, Ma, Mc, E$. These three parameters for the overall filter $H(z)$ are ω_p, ω_s, and $\Delta = \omega_s - \omega_p$, respectively.

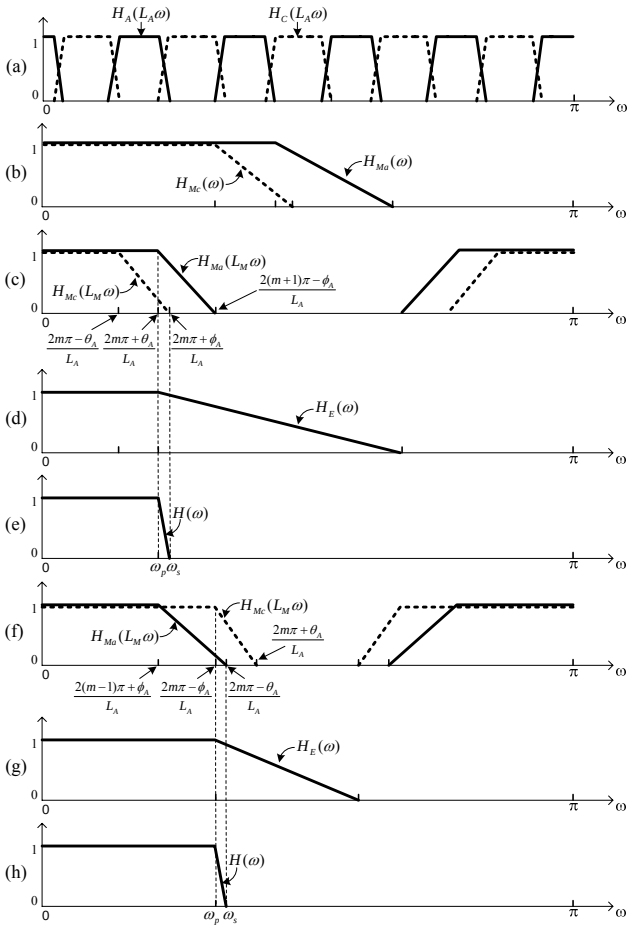

Figure 2 - Illustration of the generalized FRM approach for $L_M = 2$.

When designing the overall filter, there are two cases, namely Case A and Case B, depending on the passband widths of the masking filters. If $\theta_{Ma} > \theta_{Mc}$, the filter is a Case A design for which the parameters can be expressed as follows according to Fig. 2(c) and 2(e):[1]

$$\begin{aligned} \theta_A &= \omega_p L_A - 2m\pi \\ \phi_A &= \omega_s L_A - 2m\pi \\ m &= \lfloor \omega_p L_A/(2\pi) \rfloor, \end{aligned} \qquad (4a)$$

$$\theta_{Ma} = \frac{2m\pi + \theta_A}{L_A} L_M = \omega_p L_M, \quad \phi_{Ma} = \frac{2(m+1)\pi - \phi_A}{L_A} L_M, \qquad (4b)$$

$$\theta_{Mc} = \frac{2m\pi - \theta_A}{L_A} L_M, \qquad \phi_{Mc} = \frac{2m\pi + \phi_A}{L_A} L_M = \omega_s L_M, \qquad (4c)$$

$$\theta_E = \omega_p, \qquad \phi_E = \frac{2\pi}{L_M} - \frac{2(m+1)\pi - \phi_A}{L_A} \qquad (4d)$$

[1] $\lfloor x \rfloor$ denotes the largest integer less than or equal to x.

for some positive integer m. Similarly, if $\theta_{Ma} < \theta_{Mc}$, the filter is a Case B design whose parameters can be written as follows according to Fig. 2(f) and 2(h):[2]

$$\begin{aligned} \theta_A &= 2m\pi - \omega_s L_A \\ \phi_A &= 2m\pi - \omega_p L_A \\ m &= \lceil \omega_s L_A /(2\pi) \rceil, \end{aligned} \tag{5a}$$

$$\theta_{Ma} = \frac{2(m-1)\pi + \phi_A}{L_A} L_M, \qquad \phi_{Ma} = \frac{2m\pi - \theta_A}{L_A} L_M = \omega_s L_M, \tag{5b}$$

$$\theta_{Mc} = \frac{2m\pi - \phi_A}{L_A} L_M = \omega_p L_M, \quad \phi_{Mc} = \frac{2m\pi + \theta_A}{L_A} L_M, \tag{5c}$$

$$\theta_E = \omega_p, \qquad \phi_E = \frac{2\pi}{L_M} - \frac{2m\pi + \theta_A}{L_A}. \tag{5d}$$

2.3 Choices of L_M and L_A

In the generalized FRM approach, the complexity of the overall filter is defined by the sum of the orders of four subfilters. Since the transition-band width of an FIR filter is inversely proportional to the filter length [7], the complexity measure, C, can be expressed in terms of the transition-band widths of the subfilters as follows:

$$C = \frac{1}{\Delta_A} + \frac{1}{\Delta_{Ma}} + \frac{1}{\Delta_{Mc}} + \frac{1}{\Delta_E} \tag{6}$$

L_M and L_A are chosen to minimize C. The possible intervals given below can be useful for a good selection.

$$1 \le L_M \le \lceil \pi / \omega_s \rceil - 1 \tag{7a}$$

$$\max\left\{ \frac{\pi}{\omega_p}, \frac{4L_M\pi}{\pi + \omega_s L_M} \right\} < L_A < \frac{\pi}{\Delta} \tag{7b}$$

3. ADAPTING THE TWO-STEP OPTIMIZATION ALGORITHM TO THE GENERALIZED ONE-STAGE FRM FILTERS

In this section, it is described how to simultaneously optimize all the subfilters using in the generalized one-stage FRM approach.

3.1 Finding an Initial Solution

Given the specifications of $H(z)$, i.e. ω_p, ω_s, δ_p, and δ_s.[3] First, band edges of the subfilters and the interpolation factors (L_M and L_A) are determined by the equations (4) – (7). The orders of the subfilters can be estimated by the formula given in [7]. Second, the initial coefficients for the subfilters are found using the Remez algorithm.[4] The passband and stopband weights are $1 / \delta_p$ and $1 / \delta_s$, respectively.

[2] $\lceil x \rceil$ denotes the smallest integer larger than or equal to x.

[3] δ_p and δ_s are the passband and stopband ripples, respectively.

[4] In MATLAB, *remez.m* function can be used for this purpose.

3.2 Improving the Initial Solution

The optimization problem given by Eq. (8a) is to find the adjustable parameter vector Φ which minimizes the maximum value of the absolute error function $|E(\Phi,\omega)|$, such that

$$\min_{\Phi} \left\{ \max_{\omega \in [0,\, \omega_p] \cup [\omega_s,\, \pi]} \left| E(\Phi,\, \omega) \right| \right\}, \tag{8a}$$

where

$$\begin{aligned} \Phi = \big[& h_A(0), \ldots, h_A(N_A/2), h_{Ma}(0), \ldots, h_{Ma}\lfloor N_{Ma}/2 \rfloor, \\ & h_{Mc}(0), \ldots, h_{Mc}\lfloor N_{Mc}/2 \rfloor, h_E(0), \ldots, h_E\lfloor N_E/2 \rfloor \big], \end{aligned} \tag{8b}$$

and

$$E(\Phi,\omega) = W(\omega)[H(\Phi,\omega) - D(\omega)], \tag{8c}$$

with

$$D(\omega) = \begin{cases} 1, & \omega \in [0, \omega_p] \\ 0, & \omega \in [\omega_s, \pi] \end{cases}, \tag{8d}$$

$$W(\omega) = \begin{cases} 1/\delta_p, & \omega \in [0, \omega_p] \\ 1/\delta_s, & \omega \in [\omega_s, \pi] \end{cases}. \tag{8e}$$

Here, $H(\Phi,\omega)$ is the zero-phase frequency response of the overall transfer function $H(z)$, being a function of Φ and ω. $D(\omega)$ and $W(\omega)$ are the desired and weighting functions, respectively.

The continuous optimization problem in Eq. (8a) can be changed to a discrete minimax problem as given by Eq. (9) by decomposing of the passband and stopband regions into the frequency points $\omega_j \in [0,\omega_p]$ for j = 1, 2, . . . , J_p and $\omega_j \in [\omega_s,\pi]$ for $j = J_p+1, J_p+2, \ldots, J_p+J_s$.

$$\min_{\Phi} \left\{ \varepsilon = \max_{1 \le j \le J_p + J_s} \left| E(\Phi, \omega_j) \right| \right\} \le 1 \tag{9}$$

Hence, this problem can be solved by using an efficient unconstrained nonlinear optimization algorithm.[5]

In order to reach the best solution, i.e. the solution meeting the given criteria with the minimum number of multipliers, the above algorithms are performed for various order combinations near to the estimated orders.

3.3 Practical Filter Design

The number of frequency points, $I = J_p + J_s$, in the discrete minimax problem should be large enough to obtain good results after optimization. Otherwise, there may be spikes on the error function between two neighbouring sampling points. The proper value for the number of frequency grid points is given by $I = q \cdot N_A \cdot L_A$ for a real number $q \in [3,6]$ in [6]. The more grid points yield the more accurate final solution with a slower convergence rate. Convergence to a good solution can be accelerated by doing the optimization in the following steps:

[5] In MATLAB, *fminimax.m* function can be used for this purpose.

Step 1: Start with $k = 1$. In the region of $[0,\omega_p]\cup[\omega_s,\pi]$, determine a uniform set $\Omega_{dense} = \{\omega_1, \omega_2, \ldots, \omega_I\}$, which is dense, and in the same frequency region, select an initial uniform set $\bar{\Omega}_0 = \{\bar{\omega}_1, \bar{\omega}_2, \ldots, \bar{\omega}_J\}$, which is sparse, with $J = \lfloor I/100 \rfloor$.

Step 2: Evaluate the absolute error function $|E(\Phi,\omega_j)|$ on Ω_{dense} and determine the grid points corresponding to the local maxima of this function. In the other words, find those ω_j's in Ω_{dense} for which

$$\left|E(\Phi,\omega_{j-1})\right| < \left|E(\Phi,\omega_j)\right| > \left|E(\Phi,\omega_{j+1})\right|, \quad (10)$$

where $\left|E(\Phi,\omega_0)\right| = \left|E(\Phi,\omega_{J+1})\right| = 0$. Store these grid points into Ω_{new} and set $\bar{\Omega}_k = \bar{\Omega}_{k-1} \cup \Omega_{new}$.

Step 3: Solve the discrete minimax problem in Eq. (9) with the frequency points of $\bar{\Omega}_k$ and refresh Φ vector.

Step 4: If $\left|\bar{\Omega}_{k-1}\right| = \left|\bar{\Omega}_k\right|$, then stop.[6] Otherwise, set $k = k + 1$ and go to Step 2.

This algorithm is ended when the number of grid points remains the same between two consecutive iterations.

4. NUMERICAL EXAMPLE

In this section, the efficiency of the proposed technique is illustrated by means of an example taken from the literature.

Consider the specifications [3, 5, 8]: $\omega_p = 0.4\pi$, $\omega_s = 0.402\pi$, $\delta_p = 0.01$, and $\delta_s = 0.001$. For the optimum conventional direct-form FIR filter, the minimum order to meet the given criteria is 2541, requiring 1271 multipliers and 2541 adders when the coefficient symmetry is exploited.

For the original one-stage FRM approach [3], the number of multipliers required in the implementation is minimized by $L_A = 16$. The minimum orders for $H_{Ma}(z)$, $H_{Mc}(z)$, and $H_A(z)$ to meet the given specifications are $N_{Ma} = 70$, $N_{Mc} = 98$, and $N_A = 162$, respectively. The overall number of multipliers and adders for this design are 168 and 330, respectively, that are 13 percent of those required by an equivalent conventional direct-form design (1271 and 2541). The overall filter order is 2690, which is only 6 percent higher than that of the direct-form design (2541).

For the generalized one-stage FRM filter, according to Eq. (7a) and (7b), we have the possible intervals of L_M and L_A, such that $1 \le L_M \le 2$ and $3 \le L_A \le 499$. A search over these ranges leads to the minimum value of $C = 52.23$ with $L_M = 2$ and $L_A = 26$. For these selections, the overall filter is a Case A design with $m = 5$, $\theta_A = 0.4\pi$, and $\phi_A = 0.452\pi$. The best solution resulting when using the proposed design scheme is obtained by $N_{Ma} = 20$, $N_{Mc} = 64$, $N_E = 16$, and $N_A = 100$. For this filter, the number of multipliers and adders are 104 and 200, respectively, that are approximately 62 percent of those of the original one-stage design (168 and 330). The overall filter order increases to 2744, which is only 8 percent of that of the direct-form filter. Some of the characteristics related to the filter designs using various techniques are summarized in Table 1. Here, Π denotes the number of multipliers required to implement the overall filter.

Table 1 - Summary of designs in the example under consideration.

Method	L_A	L_M	N_A	N_{Ma}	N_{Mc}	N_E	Π
Direct-form	–	–	–	–	–	–	1271
Original FRM [3]	16	1	162	70	98	–	168
Proposed in [4]	26	2	112	66	90	38	157
Proposed in [5]	16	1	160	47	57	–	134
Proposed in [5]	21	1	122	55	77	–	129
Proposed in [8]	21	1	122	0	46	55	114
Our proposed tech.	26	2	100	20	64	16	104

For the best design by using the proposed technique with $L_M = 2$ and $L_A = 26$, the overall magnitude response with the passband details is illustrated in Figure 3. Figure 4 and 5 show the responses for $H_A(L_A\omega)$ and $1 - H_A(L_A\omega)$ as well as $H_{Ma}(L_M\omega)$ and $H_{Mc}(L_M\omega)$, respectively. The magnitude response for $H_E(\omega)$ is depicted in Figure 6. As seen in Figure 5, the similarity of the responses for $H_{Ma}(L_M\omega)$ and $H_{Mc}(L_M\omega)$ is a remarkable observation.

5. CONCLUSION

In this paper, an existing two-step optimization algorithm, recently proposed for optimizing multistage FRM filters, is applied to the generalized one-stage FRM approach. Compared to the earlier one-stage design schemes, this technique achieves further reduction in the arithmetic complexity of narrowband sharp FIR filters.

6. ACKNOWLEDGEMENT

This work was supported by the National Planning Organization of Turkey for the graduate degree programs funding advance technologies in Istanbul Technical University.

REFERENCES

[1] Y. C. Lim, "Frequency-response masking approach for the synthesis of sharp linear phase digital filters", *IEEE Trans. Circuits Syst.*, vol. CAS-33, pp. 357–364, Apr. 1986.

[2] Y. C. Lim and Y. Lian, "The optimum design of one- and two-dimensional FIR filters using the frequency response masking technique", *IEEE Trans. Circuits Syst. II*, vol. 40, pp. 88–95, Feb. 1993.

[3] T. Saramäki and Y. C. Lim, "Use of the Remez algorithm for designing FIR filters utilizing the frequency-response masking approach", in *Proc. IEEE Int. Symp. Circuits Syst.*, Orlando, FL, May 1999, pp. 449–455.

[4] R. Yang, B. Liu, and Y. C. Lim, "A new structure of sharp transition FIR filters using frequency-response masking", *IEEE Trans. Circuits Syst.*, vol. CAS-35, pp. 955–966, Aug. 1988.

[6] $|\Omega|$ denotes the size of the set Ω.

[5] T. Saramäki and H. Johansson, "Optimization of FIR filters using the frequency-response masking approach", in *Proc. IEEE Int. Symp. Circuits Syst.*, Sydney, Australia, May 2001, vol. II, pp. 177–180.

[6] J. Yli-Kaakinen, T. Saramäki, and Y. J. Yu, "An efficient algorithm for the optimization of FIR filters synthesized using the multistage frequency-response masking approach", in *Proc. IEEE Int. Symp. Circuits Syst.*, *ISCAS'04*, vol. 5, pp. 540–543, Vancouver, Canada, May 2004.

[7] O. Herrmann, L. R. Rabiner, and D. S. Chan, "Practical design rules for optimum finite impulse response lowpass digital filters", *Bell Syst. Tech. J.*, vol. 52, no. 6, pp. 769–799, July/Aug. 1973.

[8] T. Saramäki and J. Yli-Kaakinen, "Optimization of frequency-response-masking based FIR filters with reduced complexity", in *Proc. IEEE Int. Conf. Circuits Syst.*, Scottsdale, Arizona, vol. III, pp. 225–228, 2002.

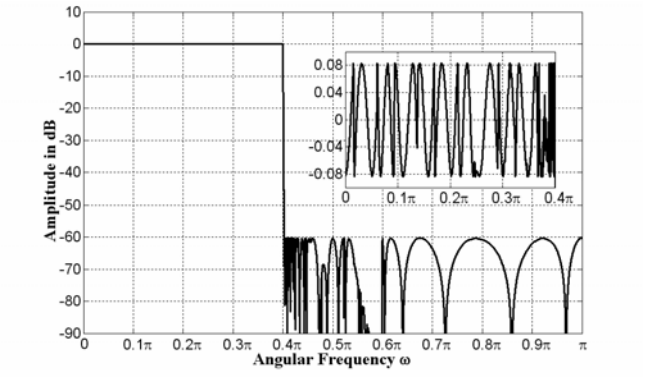

Figure 3 - Response for the best proposed overall filter for $L_M = 2$ and $L_A = 26$.

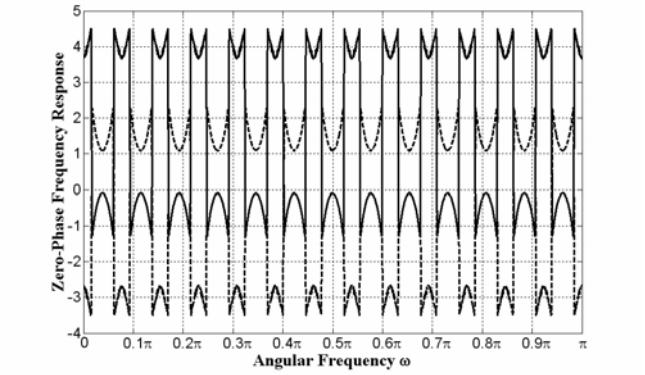

Figure 4 - Responses for $H_A(L_A\omega)$ (solid line) and $1 - H_A(L_A\omega)$ (dashed line) for $L_A = 26$.

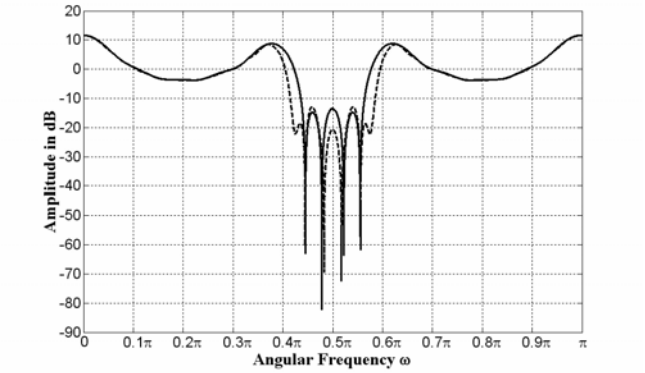

Figure 5 - Responses for $H_{Ma}(L_M\omega)$ (solid line) and $H_{Mc}(L_M\omega)$ (dashed line) for $L_M = 2$.

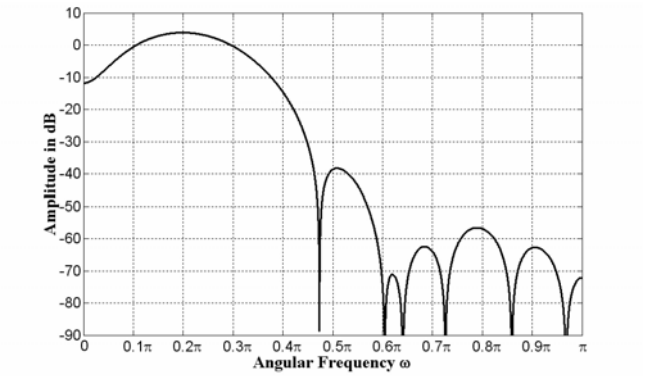

Figure 6 - Response for $H_E(\omega)$.